

PAM-Independent CRISPR-Cas12a System for Specific Assays of Single Nucleotide Variants

Jinlong Ai,^{||} Jinhai Deng,^{||} Jingjing Hu, Xingxiang Pu,^{*} Tongyan Yuan, Yuling Teng, Han Li, Bojie Chen, Jinlian Du, Ling Jiang,^{*} Xiaoyan Chen, Erhu Xiong,^{*} and Ronghua Yang



Cite This: *JACS Au* 2025, 5, 1392–1401



Read Online

ACCESS |

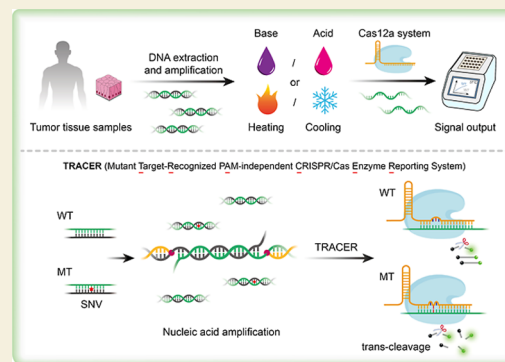
Metrics & More

Article Recommendations

Supporting Information

ABSTRACT: The CRISPR-Cas12a system has been extensively utilized in nucleic acid detection owing to its remarkable sensitivity and specificity. Nonetheless, its strict dependency on the presence of a protospacer adjacent motif (PAM) within double-stranded DNA (dsDNA) introduces considerable limitations, thereby constraining its applicability, flexibility, and broader accessibility in molecular diagnostics. Here, we communicate a universal, robust, and high-fidelity method for a PAM-independent nucleic acid assay based on the CRISPR-Cas12a system, named TRACER (mutant target-recognized PAM-independent CRISPR-Cas12a enzyme reporting system). TRACER can effectively distinguish target nucleic acids at concentrations as low as 0.5 aM, thereby enabling it to identify the presence of a 0.1% single nucleotide variant (SNV)-included mutant-type gene in heterozygotes. Thus, TRACER exhibits comparable sensitivity, specificity, and accuracy to Sanger sequencing in analyzing the SNV-related clinical tumor samples. Overall, TRACER introduces a brand-new perspective for SNV assays by eliminating the dependency on PAM sites and significantly expands the application range of the CRISPR-Cas12a system, thus holding immense potential for clinical diagnostics, biomedical research, and drug discovery.

KEYWORDS: CRISPR-Cas12a system, protospacer adjacent motif, single nucleotide variants, nucleic acid amplification, clinical diagnostics



INTRODUCTION

Cancer is one of the leading causes of death worldwide, posing significant challenges to public health and socio-economic systems.^{1,2} Early and accurate diagnostics of cancer are crucial for improving treatment effects and patient survival rates.^{3–5} Except for clinical imageological and histopathological diagnostics,⁶ nucleic acid detection has shown immense potential in cancer diagnosis and monitoring, which primarily involves the analysis of biomarkers such as gene mutations, gene rearrangements, and copy number variations.^{7,8} Single nucleotide variants (SNVs) are the most prevalent type of genomic alterations and often carry crucial clinical and biological information, thereby providing precise evidence for disease susceptibility and supporting personalized treatment strategies.^{9–14}

As the gold standard for nucleic acid detection, quantitative polymerase chain reaction (qPCR) is widely applied due to its simple design, high sensitivity, and low cost.^{15,16} However, it faces challenges in detecting subtle changes caused by SNVs, especially when they are embedded within numerous wild-type (WT) background sequences. Conventional probe designs often struggle to distinguish single base changes, leading to mutant signals being masked by a large number of WT signals, which complicates interpretation of the results. In contrast,

gene sequencing can accurately and efficiently distinguish SNVs at the genome level.^{17,18} However, its widespread application is limited by the requirement of expensive equipment, high testing costs, and lengthy analysis times, making it impractical for routine target detection. Thus, it is desirable to develop high-efficiency and low-cost strategies for SNV detection.

In recent years, CRISPR (clustered regularly interspaced short palindromic repeats) technology has been widely used in the field of molecular diagnosis due to its precise recognition ability and high specificity.^{19,20} As the most extensively studied CRISPR-associated (Cas) enzymes, Cas9, Cas12, and Cas13 effectors have different mechanisms for target recognition and substrate cleavage.^{21–25} Different from Cas9, Cas12, and Cas13 effectors, under the guidance of their CRISPR RNA (crRNA), can nonspecifically cleave surrounding single-stranded DNA (ssDNA) or ssRNA after recognizing their

Received: January 6, 2025

Revised: February 4, 2025

Accepted: February 5, 2025

Published: February 22, 2025



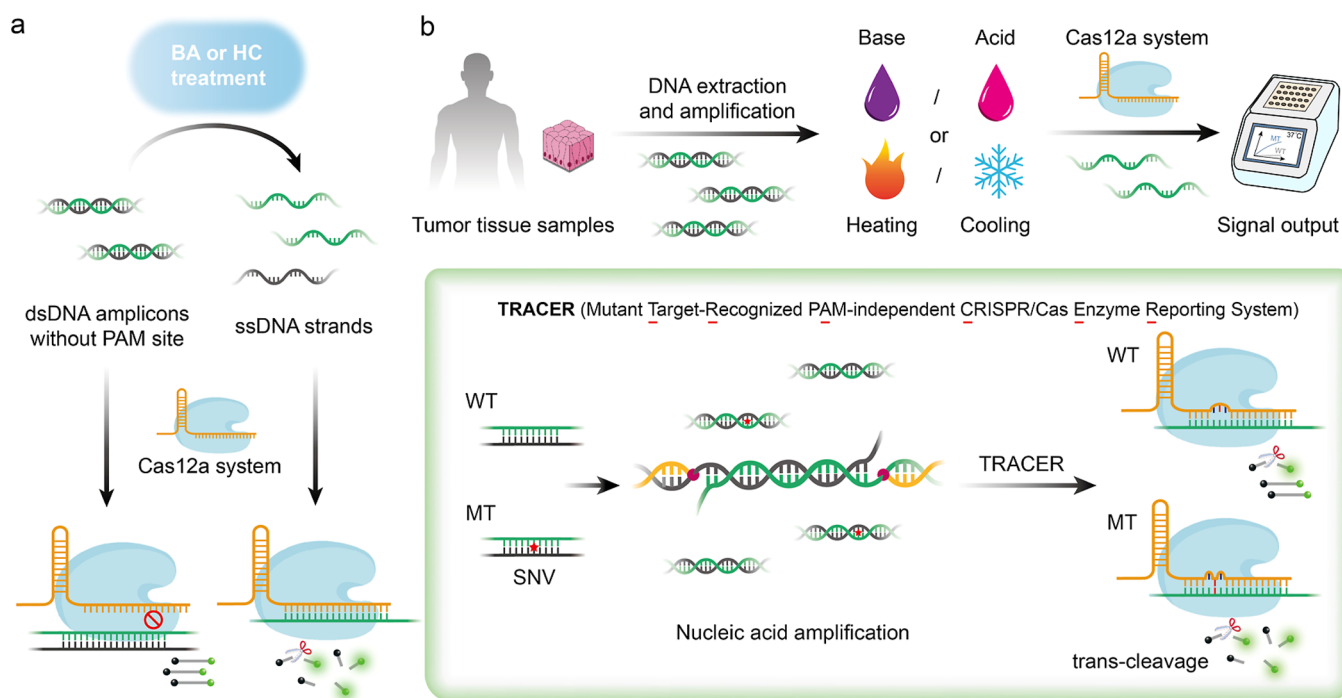


Figure 1. Principle of TRACER. (a) Schematic illustration of the conversion of dsDNA amplicons to ssDNAs. The ssDNAs can be recognized by the CRISPR-Cas12a system without the requirement for a PAM site to generate amplified fluorescence signals. (b) Genomic DNA extracted from tumor tissues is amplified by PCR or RPA and detected using the CRISPR-Cas12a system after BA or HC treatment. The WT targets fail to initiate obvious fluorescence signals due to more mismatches with crRNA.

target nucleic acids (termed *trans*-cleavage activity).^{26–30} Based on this, researchers typically label fluorescence and quenching groups at both ends of the ssDNA or ssRNA to form FQ-reporter probes. Once the CRISPR-Cas12/Cas13 system is activated by their targets, the nonspecific cleavage of the FQ reporters can generate an amplified signal, thereby significantly improving the sensitivity of molecular diagnostics.^{31–34} In contrast to the CRISPR-Cas13 system, which recognizes ssRNA targets, the CRISPR-Cas12 system can recognize both dsDNA and ssDNA targets.³⁵ When recognizing dsDNA targets, a protospacer adjacent motif (PAM) site with a specific sequence (5'-TTTV-3') near the target region is required.³⁶ However, many genetic mutation-related diseases have few PAM sites near the mutated region, especially SNVs.^{37,38} Additionally, although such a PAM site exists near the SNV, the location of the SNV may not be in the seed region recognized by the Cas12a/crRNA complex, making the CRISPR-Cas12a system insensitive to the SNV, which greatly limits its applicability, flexibility, and accessibility.³⁹ To address this issue, many efforts have been made. Zhang and co-workers performed a structure-guided protein mutagenesis screen to increase the targeting range of Cas12a, which can recognize noncanonical PAMs.⁴⁰ However, the process of protein modification and screening is complex, and the CRISPR-Cas12a system still fundamentally depends on the presence of a PAM site. Another strategy is to introduce a PAM sequence into the amplification primers, ensuring that the amplified products contain a PAM site recognized by the CRISPR-Cas12a system.⁴¹ However, this method requires strict primer design and optimization and does not get rid of the dependence on PAM sites. Chen et al. employed high temperature and T_m -lowering additives to obtain DNA bubbles for Cas12a recognition, but the introduction of T_m -lowering additives not only diminishes the affinity of the dsDNA target

but also may attenuate the binding affinity of crRNA to the dsDNA target, thereby compromising the detection efficiency.⁴² Similarly, although an artificial bubble structure in the seed region of the dsDNA target can overcome the PAM restriction, this design is tailored for the detection of enzymes, small molecules, and miRNAs and is not applicable to genomic dsDNA.⁴³ Additionally, the strategy of generating sticky-end dsDNA through temperature-mediated dsDNA unwinding and introducing helper ssDNAs improves the identification of SNVs. However, the length of the initiation region and the blocker strand sequence need to be redesigned and optimized for various targets, and the flapping process can somewhat diminish the rate of fluorescence signal generation compared to directly targeting ssDNA.⁴⁴ In contrast, the asymmetric recombinase polymerase amplification (RPA) reaction can generate full-length ssDNA, but it inevitably sacrifices the efficiency of nucleic acid amplification, leading to a decreased detection sensitivity.⁴⁵ Therefore, it is crucial to develop a new strategy to overcome the limitation of PAM sites without compromising the detection sensitivity for SNV assays.

Herein, we communicate a universal, robust, and high-fidelity method for PAM-independent SNV assays based on the CRISPR-Cas12a system, named TRACER (mutant target-recognized PAM-independent CRISPR-Cas12a enzyme reporting system) (Figure 1). In this strategy, the dsDNA products from the nucleic acid amplification reaction are unwound through the treatment of alkaline solution or high temperature to generate abundant ssDNA.⁴⁶ After neutralization with acid or cooling to a specific temperature, the ssDNAs are targeted by the CRISPR-Cas12a system without the requirement for the PAM site. Once activated, the CRISPR-Cas12a system can cleave the FQ-reporter probe to yield fluorescence signals. TRACER can effectively distinguish the target nucleic acids at concentrations as low as 0.5 aM, thereby enabling it to identify

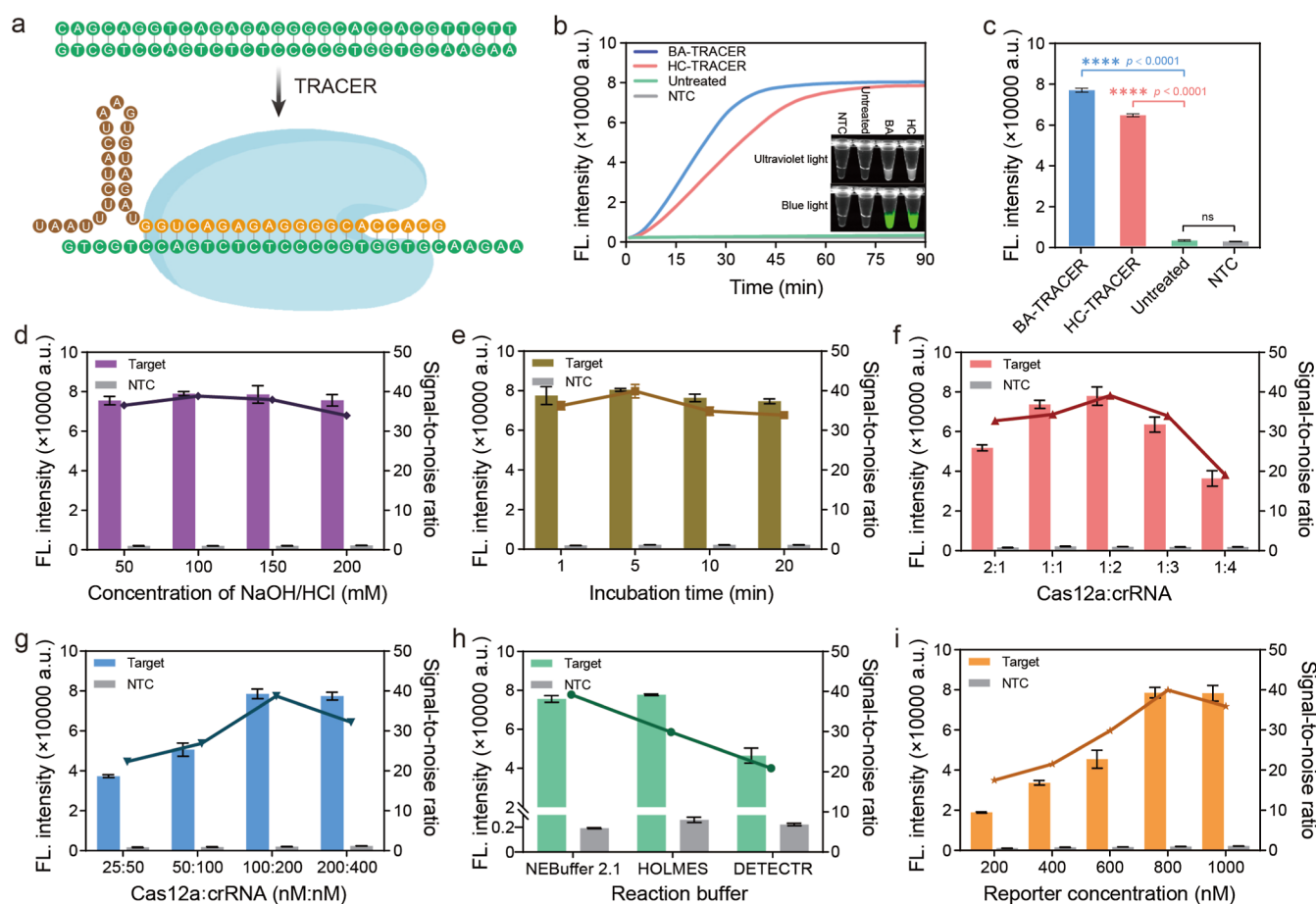


Figure 2. Feasibility and optimization of TRACER. (a) Randomly designed dsDNA sequence without a PAM site. (b) Fluorescence kinetic curves of feasibility analysis of BA- and HC-TRACER. Inset: fluorescence imaging after BA- and HC-TRACER under ultraviolet/blue light. (c) Representative fluorescence intensities at $t = 45$ min. (d–i) Optimization of the concentration of NaOH/HCl (d), incubation duration (e), ratio of Cas12a protein to crRNA (f), concentration of Cas12a protein and crRNA (g), type of reaction buffer (h), and concentration of FQ reporter (i). The end-point fluorescence intensities are plotted at $t = 45$ min. Error bars represent at least three independent experiments.

the presence of a 0.1% mutant-type (MT) gene in heterozygotes. Finally, we detected the tumor tissue samples of 27 cases of breast cancer (ESR1 gene) and 30 cases of nonsmall cell lung cancer (NSCLC, EGFR gene), which showed comparable sensitivity, specificity, and accuracy to Sanger sequencing. Overall, TRACER offers a new perspective for SNV assays that is independent of PAM sites, effectively broadening the applicability of the CRISPR-Cas12a system, and thus holds significant potential for clinical diagnostics, biomedical research, and drug discovery.

RESULTS AND DISCUSSION

Principle of TRACER

The CRISPR-Cas12a-based molecular diagnostics generally depend on the nucleic acid amplicons that contain a PAM site. This reliance significantly restricts the diversity of the sequence selection for the desired targets. Although Cas enzymes can be engineered to relax PAM recognition, thereby enhancing their targeting properties, such modifications may present challenges in applications that demand high specificity, especially in SNV assays. To address this issue, we communicated a universal, robust, and high-fidelity TRACER platform. As shown in Figure 1a, the CRISPR-Cas12a system is unable to recognize dsDNA amplicons that lack a PAM site, yet it can be effectively activated by ssDNA targets irrespective of the PAM site

requirement. Briefly, in the workflow of TRACER, genomic DNA extracted from tumor tissues is amplified by PCR or RPA. Then, the dsDNA amplicons were treated with NaOH solution or a high temperature to generate abundant ssDNAs. After neutralization with HCl (BA-TRACER) or cooling to a specific temperature (HC-TRACER), these SNV-contained ssDNAs were recognized by the CRISPR-Cas12a system, which triggered nonspecific *trans*-cleavage activity, resulting in amplified fluorescence signals (Figure 1b). However, the WT ssDNAs failed to initiate obvious fluorescence signals because of more mismatches with the crRNA, thereby ensuring the specificity of the TRACER.

Feasibility and Optimization of TRACER

Having introduced the principle of TRACER, we next verified the feasibility and optimized the experimental parameters. First, to validate the generation of ssDNA after BA or HC treatment, we designed a dsDNA labeled with a fluorophore and a quencher. After BA or HC treatment, significant fluorescence signals were observed, while the untreated dsDNA showed no signals due to the fluorescence resonance energy transfer (FRET) efficiency (Figure S1a,b). The observation suggested the conversion of dsDNA into ssDNA, which was also confirmed by polyacrylamide gel electrophoresis (PAGE) analysis (Figure S1c). Next, to further demonstrate the production of ssDNA, we designed a random

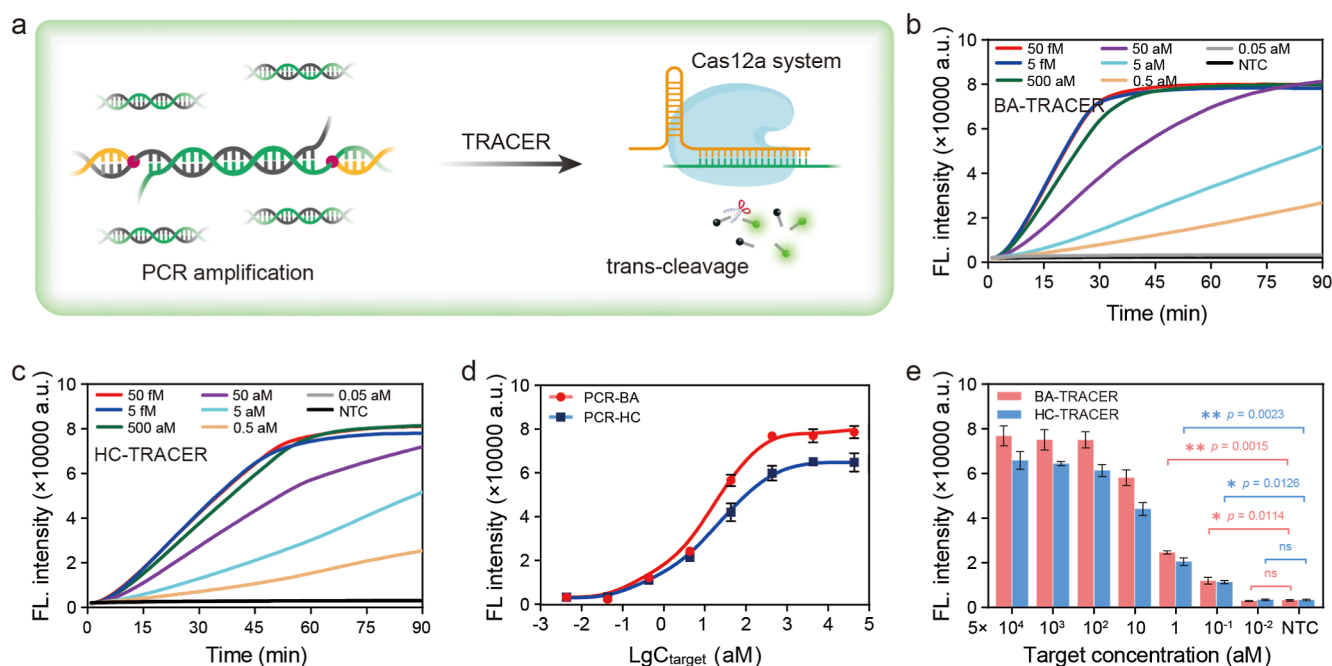


Figure 3. Sensitivity analysis of BA- and HC-TRACER. (a) Schematic diagram of target DNA amplified by PCR in the BA- and HC-TRACER. (b) Fluorescence kinetic analysis of target DNA amplified by PCR in the BA-TRACER. (c) Fluorescence kinetic analysis of target DNA amplified by PCR in the HC-TRACER. (d) Representative fluorescence intensities of the BA- and HC-TRACER. (e) Relationships between the logarithm of target concentrations and the fluorescence intensities by the BA- and HC-TRACER. The end-point fluorescence intensities are plotted at $t = 45$ min. Error bars represent at least three independent experiments.

dsDNA without a PAM site, which cannot activate the CRISPR-Cas12a system (Figure 2a). In BA- or HC-TRACER, the generation of remarkable fluorescence signals indicated the efficient conversion of dsDNA to ssDNA, which effectively activated the CRISPR-Cas12a system, enabling it to non-specifically cleave the FQ reporter (Figure 2b,c). Fluorescence imaging under ultraviolet/blue light corroborated the above results (Figure 2b). Furthermore, the PAGE results showed no distinct bands post BA- and HC-TRACER, validating that the ssDNA, derived from dsDNA treated with BA and HC, successfully activated the nonspecific ssDNA cleavage of the CRISPR-Cas12a system. This finding further substantiated the generation of ssDNA and underscored the excellent feasibility of TRACER (Figure S2). We then evaluated the catalytic activities of the CRISPR-Cas12a system in the presence of ssDNA or dsDNA with/without PAM. As shown in Figure S3, the CRISPR-Cas12a system exhibited robust catalytic activities toward both ssDNA and PAM-containing dsDNA. In contrast, dsDNA without a PAM site failed to activate the CRISPR-Cas12a system, resulting in no catalytic activity.

Subsequently, we attempted to conduct multiparametric optimizations of the BA- and HC-TRACER, encompassing various parameters such as the concentration of NaOH/HCl, incubation temperature and duration, concentration and ratio of Cas12a protein to crRNA, type of reaction buffer, FQ-reporter concentration, and so on. In the BA-TRACER, the dsDNAs were treated with a NaOH solution to facilitate denaturation, followed by the addition of HCl to neutralize the pH of the reaction system, thereby rendering it compatible for the subsequent CRISPR assay. We first investigated the concentration of NaOH/HCl and the incubation duration. As shown in Figure 2d,e, no significant variation in fluorescence intensity and signal-to-noise (S/N) ratio was observed across various concentrations of NaOH/HCl and incubation

durations. Consequently, a concentration of 50 mM NaOH/HCl and a 1 min incubation period were identified as the optimal conditions for the assay (Figure S4). Following that, several CRISPR assay-related parameters were meticulously evaluated. The results showed that with the increase of the ratio of Cas12a protein to crRNA, the fluorescence signal enhanced correspondingly, and the best ratio was 1:2 (100 nM: 200 nM) (Figures 2f,g and S5). Then, we delved into different reaction buffers, including NEBuffer 2.1, HOLMES buffer,^{31,32} and DETECTR buffer.³⁵ We noted that the fluorescence signals produced by NEBuffer 2.1 and HOLMES buffer were similar in intensity; however, NEBuffer 2.1 showed the highest S/N ratio, leading to its selection for further use (Figures 2h and S6a). Ultimately, the concentration of the FQ reporter was investigated, and the results revealed that an 800 nM concentration of the FQ reporter yielded the optimal S/N ratio (Figures 2i and S6b).

Furthermore, the experimental parameters of HC-TRACER were also carefully evaluated. Initially, the dsDNA strands were subjected to 95 °C treatment to induce denaturation. They were then rapidly transferred to a defined temperature to preserve their single-stranded conformation. Upon exploring a range of incubation temperatures, it was observed that the fluorescence signals progressively decreased as the temperature was raised from 0 to 50 °C. Significantly, the denatured ssDNA exhibited the highest S/N ratio when incubated at 0 °C (Figure S7a,b). This result is attributed to the fact that at higher temperatures, the uncoiled ssDNAs tended to reanneal into a double-stranded configuration, thereby reducing the amount of ssDNA available to activate the CRISPR-Cas12a system, which, in turn, led to diminished fluorescence signals. Next, we explored the effect of the incubation time at 0 °C on the HC-TRACER. We observed that 1 min incubation time showed the highest fluorescence signal and S/N ratio (Figure

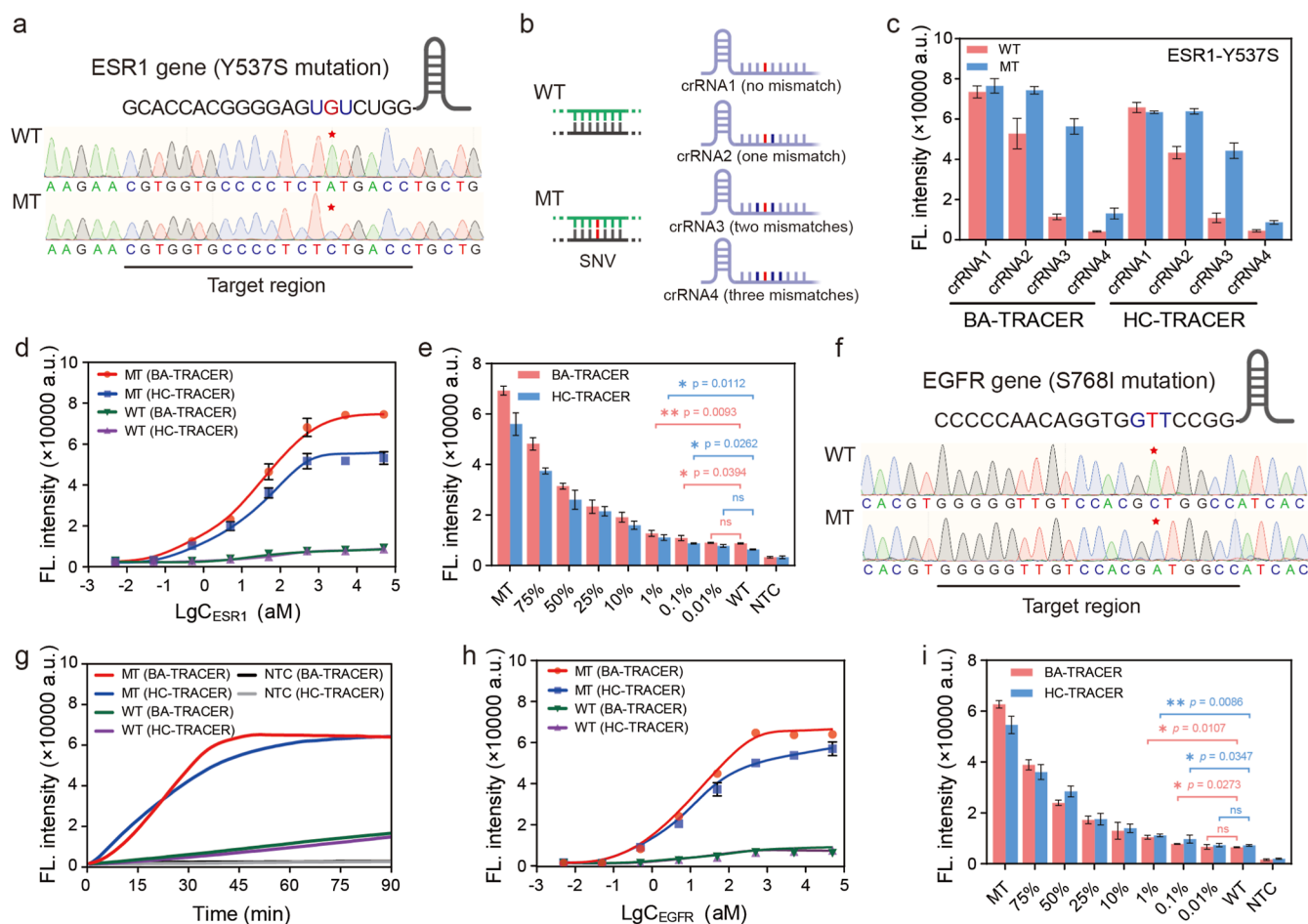


Figure 4. Analysis of SNVs by TRACER. (a) Drug-resistant ESR1-Y537S mutation in breast cancer and its corresponding crRNA. (b) Designs of various crRNAs for SNV identification. (c) Fluorescence intensities for ESR1-Y537S mutation detection using the designed four crRNAs in the BA- and HC-TRACER. (d) Detection of different concentrations of the ESR1-Y537S MT and WT genes using the crRNA3 in the BA- and HC-TRACER. (e) Detection of the mixtures with various ratios of the ESR1-Y537S MT to WT genes using the crRNA3 in the BA- and HC-TRACER. (f) EGFR-S768I mutation in NSCLC and its corresponding crRNA. (g) Fluorescence kinetic curves of the EGFR-S768I MT and WT genes using the designed crRNA in the BA- and HC-TRACER. (h) Detection of different concentrations of the EGFR-S768I MT and WT genes using the designed crRNA in the BA- and HC-TRACER. (i) Detection of the mixtures with various ratios of EGFR-S768I MT to WT genes using the designed crRNA in the BA- and HC-TRACER. The end-point fluorescence intensities are plotted at $t = 45$ min. Error bars represent at least three independent experiments.

S7c,d). Additionally, the CRISPR assay-related parameters in the HC-TRACER were also examined, and it was found that the optimal experimental conditions were largely in accordance with those of the BA-TRACER (Figures S8 and S9).

Sensitivity Analysis of TRACER

After optimization of the experimental parameters, we next proceeded to evaluate the sensitivity of TRACER under the optimal conditions (Figure 3a). Prior to that, it is essential to assess the effect of various primer pairs on the amplification efficiency of PCR and RPA. We designed three primer pairs and tested different combinations (Table S1), subsequently analyzing their amplicons using BA- or HC-TRACER. The results revealed that the F1R1 primer pair for PCR and RPA showed relatively favorable fluorescence kinetics and intensities in both BA- and HC-TRACER (Figures S10 and S11). After that, the sensitivity analysis of TRACER was performed. Initially, a series of target concentrations were utilized for PCR amplification. Then, the resulting amplicons were treated by either the BA or the HC method and subsequently detected by the CRISPR-Cas12a system. As shown in Figure 3b,c, as the

target concentration ranged from 0 to 500 aM, a notable increase in fluorescence signals was observed. Both BA- and HC-TRACER demonstrated remarkable detection capabilities, achieving a detection limit of 0.5 aM, which was much lower than that of most other techniques (Table S2). This superior sensitivity was credited to the synergistic effect of efficient PCR amplification and the powerful signal amplification afforded by the robust *trans*-cleavage activity of the CRISPR-Cas12a system (Figure 3d,e). To ascertain the impact of the nucleic acid amplification method on the analytical performance, we compared the PCR method with the RPA isothermal amplification technique, which offers the advantage of not requiring large temperature-controlled equipment. However, the results revealed that compared to the PCR method, the BA- and HC-TRACER coupled with RPA showed slower fluorescence kinetic signals and less favorable detection limits (5 aM) (Figure S12). This reduction in the detection sensitivity is likely attributable to the comparatively lower amplification efficiency of RPA.

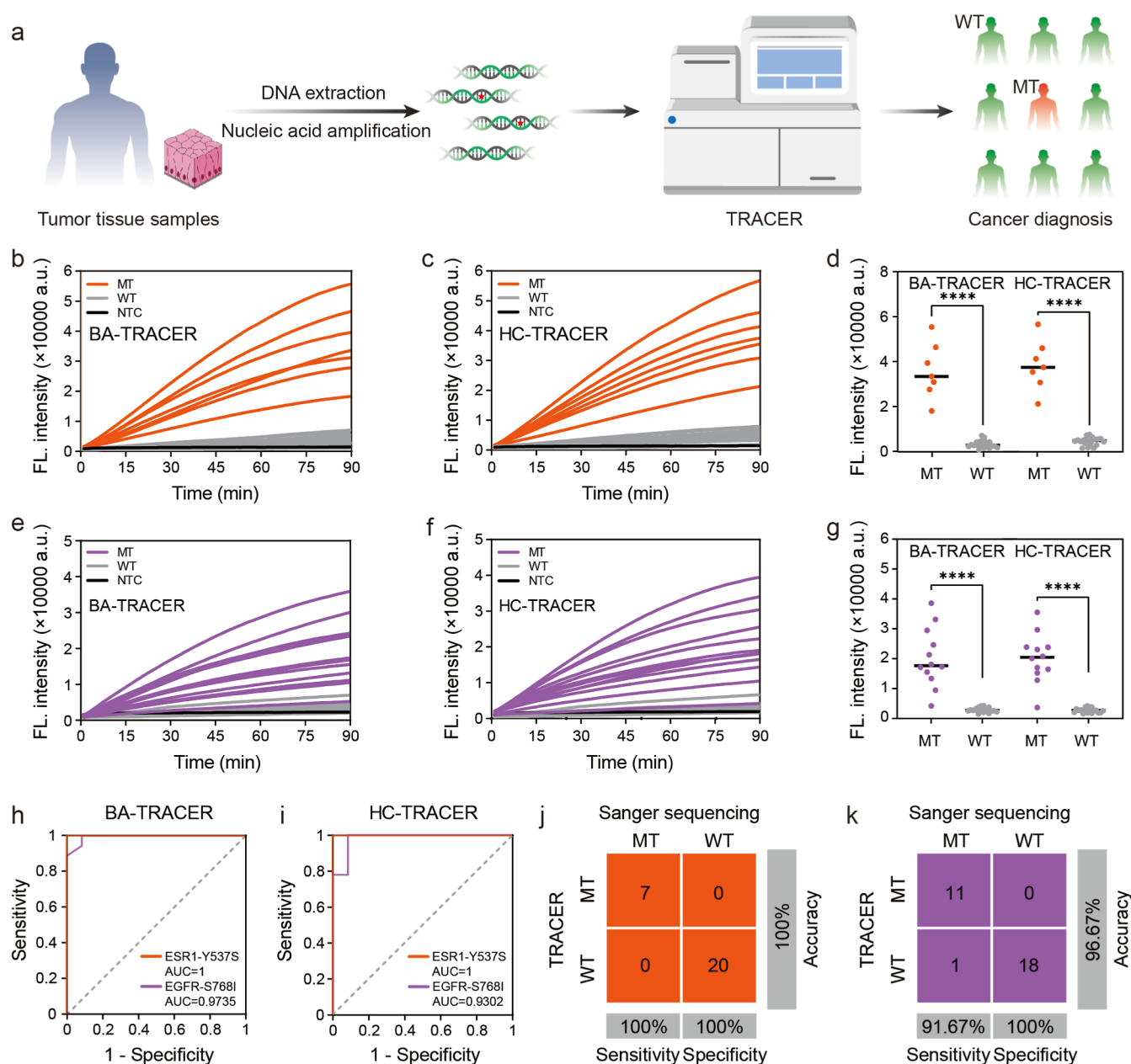


Figure 5. Clinical validation of TRACER. (a) Workflow for the detection of ESR1-Y537S and EGFR-S768I mutations in clinical samples using TRACER. (b,c) Fluorescence kinetic curves for detecting ESR1-Y537S mutation using the BA- (b) and HC-TRACER (c). (d) TRACER detection results of two clinical cohorts were obtained, including 7 of ESR1MT samples and 20 of ESR1 WT samples. Two-tailed unpaired Student's *t* tests were used to evaluate statistical differences between the ESR1-Y537S MT and WT cohorts. (e,f) Fluorescence kinetic curves for detecting EGFR-S768I mutation using the BA- (e) and HC-TRACER (f). (g) TRACER detection results of two clinical cohorts were obtained, including 12 of MT EGFR samples and 18 of WT EGFR samples. Two-tailed unpaired Student's *t* tests were used to evaluate statistical differences between the EGFR-S768I MT and WT cohorts. (h,i) ROC curves of the BA- (h) and HC-TRACER (i) for detecting ESR1-Y537S and EGFR-S768I mutations in clinical samples. (j,k) Evaluation of the clinical sensitivity, specificity, and accuracy of TRACER by comparison to Sanger sequencing using a confusion matrix.

SNV Analysis by TRACER

After thoroughly investigating the sensitivity of TRACER, we then attempted to evaluate its capability for SNV detection. As is well-known, estrogen receptor (ER)-positive breast cancer represents the largest group among breast cancer patients. The treatment for these patients often relies on endocrine therapy to regulate estrogen levels in the body, thereby controlling the disease. However, patients who rely on long-term medication often face a serious challenge: the emergence of drug resistance, which is usually associated with genetic mutations,

such as SNVs. Thus, accurately diagnosing these SNVs is crucial for the treatment of breast cancer.^{47,48} First, we assessed the ability of TRACER to identify the ESR1-Y537S mutation, which is a prevalent drug-resistant SNV in breast cancer treatment (Figure 4a). We crafted four distinct crRNAs that were thoroughly complementary to the MT gene (designated as crRNA1) and intentionally introduced one mismatch (crRNA2), two mismatches (crRNA3), or three mismatches (crRNA4), respectively, to evaluate their specificity and efficiency (Figure 4b). As shown in Figure 4c, in the BA-

and HC-TRACER assays, despite the high fluorescence signal observed, there was no significant difference in ESR1-Y537S detection when utilizing either crRNA1 or crRNA2. However, when crRNA4 was employed, the fluorescence intensities were markedly diminished for both the ESR1-Y537S MT and WT gene assays. In contrast, the specifically designed crRNA3, featuring two mismatches with the MT gene and three mismatches with the WT gene, showed a relatively distinct difference in fluorescence intensity when detecting the ESR1-Y537S MT and WT genes (Figures 4c and S13). Considering the critical importance of discrimination ability at low concentrations for practical applications, we were particularly interested in the analytical performance of BA- and HC-TRACER when utilizing the selected crRNA3. As shown in Figure 4d, both BA- and HC-TRACER could effectively discriminate between the ESR1-Y537S MT and WT genes with the assistance of crRNA3, even at exceedingly low concentrations (Figures S14 and S15). Furthermore, in actual scenarios, the proportion of the MT gene within the entire detection system is considerably low. Consequently, to evaluate the practical applicability of BA- and HC-TRACER, we prepared a series of mixtures containing various ratios of ESR1-Y537S MT to WT genes. As the proportion of the MT gene decreased, the fluorescence signals gradually weakened. Notably, even when the MT gene proportion was diminished to 0.1%, the fluorescence signal remained markedly distinguishable from that of the pure WT gene, demonstrating the capability of both BA- and HC-TRACER to detect mixtures with as little as 0.1% MT gene content (Figures 4e and S16).

To evaluate the broad applicability of the design concept, we endeavored to employ BA- and HC-TRACER to test additional SNVs. Specifically, we focused on testing the S768I mutation within the epidermal growth factor receptor (EGFR) gene, a SNV known to be a significant driver of nonsmall cell lung cancer (NSCLC) (Figure 4f).^{49,50} Utilizing the previously optimized crRNA3, we conducted subsequent tests. It was found that both BA- and HC-TRACER could effectively differentiate between the EGFR-S768I MT and WT genes, even at low concentrations, suggesting the high sensitivity and accuracy (Figures 4g,h, S17, and S18). Similarly, we also assessed the detection performance of the TRACER in identifying various ratios of EGFR-S768I MT to WT genes. The results showed that both BA- and HC-TRACER demonstrated exceptional sensitivity, enabling clear detection of mixtures containing as little as 0.1% of MT gene content (Figures 4i and S19). This implied that our TRACER is capable of precisely pinpointing the presence of any SNV, thereby facilitating more accurate diagnostics and tailored treatment recommendations for patients.

Clinical Validation of TRACER

In order to assess the clinical applicability of the BA- and HC-TRACER for distinguishing between the mutant MT and WT cancer cohorts, we collected a total of 57 tissue samples, comprising 27 samples from breast cancer patients and 30 samples from NSCLC patients, all ethically from Hunan Cancer Hospital. Compliant with the stringent medical ethical guidelines and experimental protocols, we ensured the precision and dependability of our findings. As shown in Figure 5a, as an initial step, nucleic acids were meticulously extracted from the tissue samples using a commercial column extraction kit, followed by nucleic acid amplification through PCR (Figures S20 and S21). Thereafter, the amplicons were

treated with either the BA or HC method prior to the detection using the CRISPR-Cas12a system, facilitating the differentiation between the MT and WT cohorts. As designed, our primary focus was the identification of ESR1-Y537S (breast cancer) and EGFR-S768I (NSCLC) mutations. Prior to subjecting these samples to TRACER, we conducted Sanger sequencing to verify their genetic profiles. The sequencing results revealed the presence of the ESR1-Y537S mutation in 7 out of the 27 breast cancer samples and the EGFR-S768I mutation in 12 out of the 30 NSCLC samples (Figures S22–S25). Next, we adopted BA- and HC-TRACER to identify these cancer samples. As shown in Figure 5b–d, both BA- and HC-TRACER demonstrated remarkable efficacy, successfully identifying all breast cancer samples with the ESR1-Y537S mutation. For the analysis of NSCLC samples, TRACER successfully detected nearly all EGFR-S768I mutated samples, with only one exception that remained undetected, which could potentially be attributed to the low content of the sample or its degradation (Figure 5e–g). The optimal cutoff values for both ESR1-Y537S and EGFR-S768I mutations in the BA- and HC-TRACER were determined by using receiver operating characteristic (ROC) curve analysis (Figure 5h,i). Finally, the performance of TRACER was benchmarked against Sanger sequencing using a confusion matrix analysis. The platforms demonstrated exceptional proficiency in detecting the ESR1-Y537S mutation, achieving perfect scores for sensitivity, specificity, and accuracy at 100%. In the case of the EGFR-S768I mutation, the assays also exhibited remarkable effectiveness, with a sensitivity of 91.67%, a specificity of 100%, and an overall accuracy of 96.67% (Figure 5j,k). Notably, our study did not encounter any false positives, highlighting the robustness and reliability of TRACER in the detection of genetic mutations.

CONCLUSIONS

SNVs are essential biomarkers for precision medicine, and their detection plays a multifaceted and crucial role in cancer treatment, ranging from aiding diagnosis and guiding therapy to predicting drug responses, monitoring disease progression, and assessing prognosis, all of which are integral components of precision medicine. Nevertheless, achieving precise SNV detection using CRISPR technology poses a significant challenge, especially in genomic regions devoid of accessible PAM sites. Despite this, our research aims to address these limitations, striving to enhance the accuracy and reliability of SNV detection, which is vital for the advancement of personalized cancer care.

Herein, we communicated a robust CRISPR-Cas12a-based SNV detection system, termed TRACER, which facilitated flexible and accessible nucleic acid detection without the requirement for a PAM site. In this study, we designed two dsDNA denaturation strategies (BA and HC) to generate abundant ssDNAs, thereby enabling efficient recognition by the CRISPR-Cas12a system. Under optimal conditions, both BA- and HC-TRACER can effectively detect the target concentration as low as 0.5 aM without reliance on the PAM sites, suggesting their high sensitivity. Furthermore, to enable TRACER to accurately distinguish SNVs, we meticulously designed and screened an array of crRNAs, strategically introducing base mismatches within the spacer region of crRNA. Guided by the selected crRNA, TRACER indicated efficient and precise discrimination between the MT and WT genes. The clinical utility of TRACER was further

substantiated by their successful detection of ESR1-Y537S and EGFR-S768I mutations from clinical tissue samples, which are linked to breast cancer and NSCLC, respectively. The results showed considerable clinical concordance with those obtained from Sanger sequencing, highlighting the immense potential for practical application in clinical settings.

Compared to the previous studies, although the core concept is to generate full-length or partial ssDNA recognized by the CRISPR-Cas12 system, TRACER does not affect the binding efficiency of crRNA to target nucleic acid during the detection process due to the addition of extra reagents or blocker strands, and the efficiency of nucleic acid amplification is not impacted by the asymmetry in primer concentration. Despite the encouraging results of our research, it would be an oversight not to acknowledge their inherent limitations. First, the whole detection process encompasses multiple steps, which can potentially increase the duration and complexity of the assay. This underscores the importance of optimizing each step to streamline the workflow and ensure efficient yet accurate results. Second, the transfer and treatment of amplicons can elevate the risk of aerosol contamination, potentially leading to false-positive results. Third, the current validation of TRACER is limited by a relatively small cohort of clinical tissue samples. Access to a larger set of high-quality samples for assessment could substantially bolster the demonstrated robustness and precision of TRACER. In future studies, we aim to refine a CRISPR-Cas12a-based one-pot assay, enabling the PAM-independent nucleic acid detection, which will greatly streamline the experimental procedure and eliminate the risk of aerosol contamination.

Collectively, we have discovered a universal, robust, and high-fidelity platform for nucleic acid detection that not only gets rid of the need for PAM sites in the CRISPR-Cas12a system but also offers a fresh perspective in the realm of SNV detection. Consequently, we are confident that TRACER could serve as a valuable tool for precision medicine, aiding in the selection of targeted therapeutic strategies for patients with these genetic mutations.

METHODS

Nucleic Acid Hybridization

100 μ L sample of hybridization solution, including two complementary DNA strands (10 μ M) and 1 \times NEBuffer 2.1, was incubated at 95 $^{\circ}$ C for 5 min and then cooled to 25 $^{\circ}$ C at a rate of 2 $^{\circ}$ C/min.

Polymerase Chain Reaction

The PCR reaction volume was 50 μ L, including 0.4 μ M forward primer and reverse primer, 1 \times TaqMix, various concentrations of target, and RNase-free water. The thermal cycling program: 95 $^{\circ}$ C for 5 min, followed by 35 cycles of amplification at 95 $^{\circ}$ C for 10 s, 58 $^{\circ}$ C (ESR1 gene)/52 $^{\circ}$ C (EGFR gene) for 30 s, and 72 $^{\circ}$ C for 1 min, and finally, an extension at 72 $^{\circ}$ C for 10 min and an infinite hold at 10 $^{\circ}$ C. The PCR products were stored at 4 $^{\circ}$ C for future use.

Recombinase Polymerase Amplification

The RPA reaction volume was 50 μ L, including 0.4 μ M of forward primer and reverse primer, RPA mixture, magnesium acetate (280 mM), various concentrations of target, and RNase-free water. The reaction system was incubated at 37 $^{\circ}$ C for 30 min, and the amplicons were stored at 4 $^{\circ}$ C for future use.

BA-TRACER

Two μ L portion of amplicons was added to 1 μ L of 100 mM NaOH solution to establish an alkaline environment that facilitates the unwinding of dsDNA, followed by the addition of 1 μ L of 100 mM HCl solution to neutralize the pH, ensuring compatibility with the

CRISPR-Cas12a system. Twenty μ L of the CRISPR-Cas12a system includes 100 nM Cas12a, 200 nM crRNA, 1 \times NEBuffer 2.1, unwound ssDNA, and 800 nM FQ reporter. The reaction system described above was transferred to a fluorescence plate reader and monitored on a Thermal Cycler Dice Real Time System III (TaKaRa) at 37 $^{\circ}$ C for 90 min.

HC-TRACER

Two μ L of amplicons was subjected to a thermal treatment at 95 $^{\circ}$ C for 5 min to promote the unwinding of dsDNA. Following this, the resulting amplicons were rapidly cooled to 0 $^{\circ}$ C for 1 min to preserve the ssDNAs in their unwound state. Twenty μ L of the CRISPR-Cas12a system includes 100 nM Cas12a, 200 nM crRNA, 1 \times NEBuffer 2.1, unwound ssDNA, and 800 nM FQ reporter. The above reaction system was transferred to a fluorescence plate reader and monitored on a Thermal Cycler Dice Real Time System III (TaKaRa) at 37 $^{\circ}$ C for 90 min.

Nucleic Acid Extraction from Clinical Tumor Samples

The process of nucleic acid extraction follows the instructions of the TIANquick FFPE DNA kit for the rapid nucleic acid extraction of paraffin-embedded tissue. Briefly, 30 mg of tumor sample was put in a 1.5 mL centrifuge tube, followed by the addition of 500 μ L of GL lysate and 50 μ L of GP buffer. After violent vortexing for 10 s, the sample was incubated at 98 $^{\circ}$ C for 30 min until it was dissolved. Subsequently, the nucleic acids were extracted from the above-treated sample by using the TIANquick FFPE DNA kit. Finally, the extracted genomic DNA was stored at -20 $^{\circ}$ C for future use.

PAGE Analysis

Two μ L of nucleic acid amplification products was mixed with 3 μ L of water and 1 μ L of 6 \times loading buffer, and then these mixtures were run on 8% native PAGE at 70 V for 60 min. After electrophoresis, the gels were stained with GelRed. Finally, the gels were imaged by using a GelDoc Go imaging system (Bio-Rad, USA).

ASSOCIATED CONTENT

Supporting Information

The Supporting Information is available free of charge at <https://pubs.acs.org/doi/10.1021/jacsau.5c00011>.

Materials and reagents; apparatus and instruments; ethical approval; fluorescence and PAGE analysis results; catalytic activity results; fluorescence kinetic curves; optimization of the incubation temperature and time; optimization of the concentration ratio; optimization of reaction buffer and FQ-reporter concentration; optimization of PCR and RPA primers; sensitivity analysis results; optimization of crRNA with different base mismatches; detection of the mixtures with various ratios; Sanger sequencing results; nucleic acid sequences used in this work; and comparison of various analytical techniques (PDF)

AUTHOR INFORMATION

Corresponding Authors

Xingxiang Pu – Department of Medical Oncology, Lung Cancer and Gastrointestinal Unit, Hunan Cancer Hospital & The Affiliated Cancer Hospital of Xiangya School of Medicine, Central South University, Changsha 410013, China; Email: puxingxiang@hnca.org.cn

Ling Jiang – Key Laboratory of Chemical Biology & Traditional Chinese Medicine Research (Ministry of Education), Institute of Interdisciplinary Studies, College of Chemistry and Chemical Engineering, Hunan Normal University, Changsha 410081, China; Email: ljiang630@163.com

Erhu Xiong – Key Laboratory of Chemical Biology & Traditional Chinese Medicine Research (Ministry of Education), Institute of Interdisciplinary Studies, College of Chemistry and Chemical Engineering, Hunan Normal University, Changsha 410081, China; orcid.org/0000-0002-9085-1858; Email: xiongerhu2008@163.com

Authors

Jinlong Ai – Key Laboratory of Chemical Biology & Traditional Chinese Medicine Research (Ministry of Education), Institute of Interdisciplinary Studies, College of Chemistry and Chemical Engineering, Hunan Normal University, Changsha 410081, China

Jinhai Deng – Richard Dumbleby Laboratory of Cancer Research, School of Cancer & Pharmaceutical Sciences, King's College London, London SE1 1UL, U.K.

Jingjing Hu – Key Laboratory of Chemical Biology & Traditional Chinese Medicine Research (Ministry of Education), Institute of Interdisciplinary Studies, College of Chemistry and Chemical Engineering, Hunan Normal University, Changsha 410081, China

Tongyan Yuan – Key Laboratory of Chemical Biology & Traditional Chinese Medicine Research (Ministry of Education), Institute of Interdisciplinary Studies, College of Chemistry and Chemical Engineering, Hunan Normal University, Changsha 410081, China

Yuling Teng – Key Laboratory of Chemical Biology & Traditional Chinese Medicine Research (Ministry of Education), Institute of Interdisciplinary Studies, College of Chemistry and Chemical Engineering, Hunan Normal University, Changsha 410081, China

Han Li – Key Laboratory of Chemical Biology & Traditional Chinese Medicine Research (Ministry of Education), Institute of Interdisciplinary Studies, College of Chemistry and Chemical Engineering, Hunan Normal University, Changsha 410081, China

Bojie Chen – Key Laboratory of Chemical Biology & Traditional Chinese Medicine Research (Ministry of Education), Institute of Interdisciplinary Studies, College of Chemistry and Chemical Engineering, Hunan Normal University, Changsha 410081, China

Jinlian Du – Key Laboratory of Chemical Biology & Traditional Chinese Medicine Research (Ministry of Education), Institute of Interdisciplinary Studies, College of Chemistry and Chemical Engineering, Hunan Normal University, Changsha 410081, China

Xiaoyan Chen – Department of Medical Oncology, Lung Cancer and Gastrointestinal Unit, Hunan Cancer Hospital & The Affiliated Cancer Hospital of Xiangya School of Medicine, Central South University, Changsha 410013, China

Ronghua Yang – Key Laboratory of Chemical Biology & Traditional Chinese Medicine Research (Ministry of Education), Institute of Interdisciplinary Studies, College of Chemistry and Chemical Engineering, Hunan Normal University, Changsha 410081, China; orcid.org/0000-0001-7873-6892

Complete contact information is available at: <https://pubs.acs.org/10.1021/jacsau.5c00011>

Author Contributions

[†]J.A. and J.D. contributed equally to this work.

Notes

The authors declare no competing financial interest.

ACKNOWLEDGMENTS

This work was supported by the National Natural Science Foundation of China (22274046 and 22334005), the Science and Technology Innovation Program of Hunan Province (2022RC1114), the Outstanding Youth Foundation of Hunan Provincial Education Department (24B0078), and the Hunan Provincial Innovation Foundation for Postgraduate (CX20240533).

REFERENCES

- (1) Bray, F.; Laversanne, M.; Weiderpass, E.; Soerjomataram, I. The ever-increasing importance of cancer as a leading cause of premature death worldwide. *Cancer* **2021**, *127*, 3029–3030.
- (2) Mani, K.; Deng, D.; Lin, C.; Wang, M.; Hsu, M. L.; Zaorsky, N. G. Causes of death among people living with metastatic cancer. *Nat. Commun.* **2024**, *15*, 1519.
- (3) Afrasiabi, K.; Linskey, M. E.; Zhou, Y. Exploiting Cancer's tactics to make cancer a manageable chronic disease. *Cancers* **2020**, *12*, 1649.
- (4) Crosby, D.; Bhatia, S.; Brindle, K. M.; Coussens, L. M.; Dive, C.; Emberton, M.; Esener, S.; Fitzgerald, R. C.; Gambhir, S. S.; Kuhn, P.; Rebbeck, T. R.; Balasubramanian, S. Early detection of cancer. *Science* **2022**, *375*, No. eaay9040.
- (5) Shin, H.; Choi, B. H.; Shim, O.; Kim, J.; Park, Y.; Cho, S. K.; Kim, H. K.; Choi, Y. Single test-based diagnosis of multiple cancer types using exosome-SERS-AI for early stage cancers. *Nat. Commun.* **2023**, *14*, 1644.
- (6) Zhang, M.; Wong, S. W.; Wright, J. N.; Wagner, M. W.; Toescu, S.; Han, M.; Tam, L. T.; Zhou, Q.; Ahmadian, S. S.; Shpanskaya, K.; et al. MRI radiogenomics of pediatric medulloblastoma: a multicenter study. *Radiology* **2022**, *304*, 406–416.
- (7) Dai, Y.; Wu, Y.; Liu, G.; Gooding, J. J. CRISPR mediated biosensing toward understanding cellular biology and point-of-care diagnosis. *Angew. Chem., Int. Ed.* **2020**, *59*, 20754–20766.
- (8) Pacesa, M.; Pelea, O.; Jinek, M. Past, present, and future of CRISPR genome editing technologies. *Cell* **2024**, *187*, 1076–1100.
- (9) Xiong, E.; Liu, P.; Deng, R.; Zhang, K.; Yang, R.; Li, J. Recent advances in enzyme-free and enzyme-mediated single-nucleotide variation assay in vitro. *Natl. Sci. Rev.* **2024**, *11*, nwae118.
- (10) Govindan, R.; Ding, L.; Griffith, M.; Subramanian, J.; Dees, N. D.; Kanchi, K. L.; Maher, C. A.; Fulton, R.; Fulton, L.; Wallis, J.; et al. Genomic landscape of non-small cell lung cancer in smokers and never-smokers. *Cell* **2012**, *150*, 1121–1134.
- (11) Passaro, A.; Al Bakir, M.; Hamilton, E. G.; Diehn, M.; André, F.; Roy-Chowdhuri, S.; Mountzios, G.; Wistuba, I. I.; Swanton, C.; Peters, S. Cancer biomarkers: Emerging trends and clinical implications for personalized treatment. *Cell* **2024**, *187*, 1617–1635.
- (12) Wang, G. A.; Xie, X.; Mansour, H.; Chen, F.; Matamoros, G.; Sanchez, A. L.; Fan, C.; Li, F. Expanding detection windows for discriminating single nucleotide variants using rationally designed DNA equalizer probes. *Nat. Commun.* **2020**, *11*, 5473.
- (13) Guo, C.; Deng, H.; Wang, G. A.; Huang, D.; Deng, H.; Shen, C.; Li, F.; Shen, C.; Wang, G. A.; Li, F. Coding intrinsic disorder into DNA hybridization probes enables discrimination of single nucleotide variants over wide and tunable temperature ranges. *Angew. Chem., Int. Ed.* **2023**, *62*, No. e202314386.
- (14) Huang, D.; Deng, H.; Zhou, J.; Wang, G. A.; Lei, Q.; Guo, C.; Peng, W.; Liang, P.; Shen, C.; Ying, B.; Li, Q.; Li, F. Mismatch-guided deoxyribonucleic acid assembly enables ultrasensitive and multiplex detection of low-allele-fraction variants in clinical samples. *J. Am. Chem. Soc.* **2023**, *145*, 20412–20421.
- (15) Juang, D. S.; Juang, T. D.; Dudley, D. M.; Newman, C. M.; Accola, M. A.; Rehauer, W. M.; Friedrich, T. C.; O'Connor, D. H.; Beebe, D. J. Oil immersed lossless total analysis system for integrated

RNA extraction and detection of SARS-CoV-2. *Nat. Commun.* **2021**, *12*, 4317.

(16) Fang, X.; Zhao, R.; Wang, Y.; Sun, M.; Xu, J.; Long, S.; Mo, J.; Liu, H.; Li, X.; Wang, F.; Zhou, X.; Weng, X. A bisulfite-assisted and ligation-based qPCR amplification technology for locus-specific pseudouridine detection at base resolution. *Nucleic Acids Res.* **2024**, *52*, No. e49.

(17) Xu, F.; Wang, W.; Wang, P.; Jun Li, M.; Chung Sham, P.; Wang, J. A fast and accurate SNP detection algorithm for next-generation sequencing data. *Nat. Commun.* **2012**, *3*, 1258.

(18) Aravanis, A. M.; Lee, M.; Klausner, R. D. Next-generation sequencing of circulating tumor DNA for early cancer detection. *Cell* **2017**, *168*, 571–574.

(19) Wan, Y.; Zong, C.; Li, X.; Wang, A.; Li, Y.; Yang, T.; Bao, Q.; Dubow, M.; Yang, M.; Rodrigo, L.; Mao, C. New insights for biosensing: Lessons from microbial defense systems. *Chem. Rev.* **2022**, *122*, 8126–8180.

(20) Weng, Z.; You, Z.; Yang, J.; Mohammad, N.; Lin, M.; Wei, Q.; Gao, X.; Zhang, Y. CRISPR-Cas biochemistry and CRISPR-based molecular diagnostics. *Angew. Chem., Int. Ed.* **2023**, *62*, No. e202214987.

(21) Tang, Y.; Gao, L.; Feng, W.; Guo, C.; Yang, Q.; Li, F.; Le, X. C. The CRISPR-Cas toolbox for analytical and diagnostic assay development. *Chem. Soc. Rev.* **2021**, *50*, 11844–11869.

(22) Cai, W.; Luo, T.; Mao, L.; Wang, M. Spatiotemporal delivery of CRISPR/Cas9 genome editing machinery using stimuli-responsive vehicles. *Angew. Chem., Int. Ed.* **2021**, *60*, 8596–8606.

(23) Yan, W. X.; Hunnewell, P.; Alfonse, L. E.; Carte, J. M.; Keston-Smith, E.; Sothiselvam, S.; Garrity, A. J.; Chong, S.; Makarova, K. S.; Koonin, E. V.; Cheng, D. R.; Scott, D. A. Functionally diverse type V CRISPR-Cas systems. *Science* **2019**, *363*, 88–91.

(24) Xu, C.; Zhou, Y.; Xiao, Q.; He, B.; Geng, G.; Wang, Z.; Cao, B.; Dong, X.; Bai, W.; Wang, Y.; Wang, X.; Zhou, D.; Yuan, T.; Huo, X.; Lai, J.; Yang, H. Programmable RNA editing with compact CRISPR-Cas13 systems from uncultivated microbes. *Nat. Methods* **2021**, *18*, 499–506.

(25) Liu, P.; Zeng, J.; Jiang, C.; Du, J.; Jiang, L.; Li, S.; Zeng, F.; Xiong, E. Poly (vinylpyrrolidone)-enhanced CRISPR-Cas system for robust nucleic acid diagnostics. *Anal. Chem.* **2024**, *96*, 15797–15807.

(26) Jinek, M.; Chylinski, K.; Fonfara, I.; Hauer, M.; Doudna, J. A.; Charpentier, E. A programmable dual-RNA-guided DNA endonuclease in adaptive bacterial immunity. *Science* **2012**, *337*, 816–821.

(27) Li, Y.; Mansour, H.; Watson, C. J. F.; Tang, Y.; MacNeil, A.; Li, F. Amplified detection of nucleic acids and proteins using an isothermal proximity CRISPR Cas12a assay. *Chem. Sci.* **2021**, *12*, 2133–2137.

(28) Liu, P.; Lin, Y.; Zhuo, X.; Zeng, J.; Chen, B.; Zou, Z.; Liu, G.; Xiong, E.; Yang, R. Universal crRNA acylation strategy for robust photo-initiated one-pot CRISPR-Cas12a nucleic acid diagnostics. *Angew. Chem., Int. Ed.* **2024**, *63*, No. e202401486.

(29) Cox, D. B.; Gootenberg, J. S.; Abudayyeh, O. O.; Franklin, B.; Kellner, M. J.; Joung, J.; Zhang, F. RNA editing with CRISPR-Cas13. *Science* **2017**, *358*, 1019–1027.

(30) Jiang, L.; Du, J.; Xu, H.; Zhuo, X.; Ai, J.; Zeng, J.; Yang, R.; Xiong, E. Ultrasensitive CRISPR/Cas13a-mediated photoelectrochemical biosensors for specific and direct assay of miRNA-21. *Anal. Chem.* **2023**, *95*, 1193–1200.

(31) Li, S. Y.; Cheng, Q. X.; Wang, J. M.; Li, X. Y.; Zhang, Z. L.; Gao, S.; Cao, R. B.; Zhao, G. P.; Wang, J. CRISPR-Cas12a-assisted nucleic acid detection. *Cell Discov.* **2018**, *4*, 20.

(32) Li, L.; Li, S.; Wu, N.; Wu, J.; Wang, G.; Zhao, G.; Wang, J. HOLMESv2: a CRISPR-Cas12b-assisted platform for nucleic acid detection and DNA methylation quantitation. *ACS Synth. Biol.* **2019**, *8*, 2228–2237.

(33) Gootenberg, J. S.; Abudayyeh, O. O.; Lee, J. W.; Essletzbichler, P.; Dy, A. J.; Joung, J.; Verdine, V.; Donghia, N.; Daringer, N. M.; Freije, C. A.; et al. Nucleic acid detection with CRISPR-Cas13a/C2c2. *Science* **2017**, *356*, 438–442.

(34) Liu, L.; Li, X.; Wang, J.; Wang, M.; Chen, P.; Yin, M.; Li, J.; Sheng, G.; Wang, Y. Two distant catalytic sites are responsible for C2c2 RNase activities. *Cell* **2017**, *168*, 121–134.

(35) Chen, J. S.; Ma, E.; Harrington, L. B.; Da Costa, M.; Tian, X.; Palefsky, J. M.; Doudna, J. A. CRISPR-Cas12a target binding unleashes indiscriminate single-stranded DNase activity. *Science* **2018**, *360*, 436–439.

(36) Karvelis, T.; Bigelyte, G.; Young, J. K.; Hou, Z.; Zedaveinyte, R.; Budre, K.; Paulraj, S.; Djukanovic, V.; Gasior, S.; Silanskas, A.; Venclovas, C.; Siksnys, V. PAM recognition by miniature CRISPR–Cas12f nucleases triggers programmable double-stranded DNA target cleavage. *Nucleic Acids Res.* **2020**, *48*, 5016–5023.

(37) Zhou, S.; Dong, J.; Deng, L.; Wang, G.; Yang, M.; Wang, Y.; Huo, D.; Hou, C. Endonuclease-assisted PAM-free recombinase polymerase amplification coupling with CRISPR/Cas12a (E-PfRPA/Cas) for sensitive detection of DNA methylation. *ACS Sens.* **2022**, *7*, 3032–3040.

(38) Wu, Y.; Luo, W.; Weng, Z.; Guo, Y.; Yu, H.; Zhao, R.; Zhang, L.; Zhao, J.; Bai, D.; Zhou, X.; Song, L.; Chen, K.; Li, J.; Yang, Y.; Xie, G. PAM-free CRISPR/Cas12a ultra-specific activation mode based on toehold-mediated strand displacement and branch migration. *Nucleic Acids Res.* **2022**, *50*, 11727–11737.

(39) Toth, E.; Varga, E.; Kulcsár, P. I.; Kocsis-Jutka, V.; Krausz, S. L.; Nyeste, A.; Welker, Z.; Huszár, K.; Ligeti, Z.; Tálás, A.; Welker, E. Improved LbCas12a variants with altered PAM specificities further broaden the genome targeting range of Cas12a nucleases. *Nucleic Acids Res.* **2020**, *48*, 3722–3733.

(40) Gao, L.; Cox, D. B.; Yan, W. X.; Manteiga, J. C.; Schneider, M. W.; Yamano, T.; Nishimasu, H.; Nureki, O.; Crosetto, N.; Zhang, F. Engineered Cpf1 variants with altered PAM specificities. *Nat. Biotechnol.* **2017**, *35*, 789–792.

(41) Chen, Y.; Mei, Y.; Jiang, X. Universal and high-fidelity DNA single nucleotide polymorphism detection based on a CRISPR/Cas12a biochip. *Chem. Sci.* **2021**, *12*, 4455–4462.

(42) Chen, K.; Dai, L.; Zhao, J.; Deng, M.; Song, L.; Bai, D.; Wu, Y.; Zhou, X.; Yang, Y.; Yang, S.; Zhao, L.; Chen, X.; Xie, G.; et al. Temperature-boosted PAM-less activation of CRISPR-Cas12a combined with selective inhibitors enhances detection of SNVs with VAFs below 0.01%. *Talanta* **2023**, *261*, 124674.

(43) Chen, S.; Wang, R.; Peng, S.; Xie, S.; Lei, C.; Huang, Y.; Nie, Z. PAM-less conditional DNA substrates leverage trans-cleavage of CRISPR-Cas12a for versatile live-cell biosensing. *Chem. Sci.* **2022**, *13*, 2011–2020.

(44) Zhang, W.; Mu, Y.; Dong, K.; Zhang, L.; Yan, B.; Hu, H.; Liao, Y.; Zhao, R.; Shu, W.; Ye, Z.; Lu, Y.; Wan, C.; Sun, Q.; Li, L.; Wang, H.; Xiao, X. PAM-independent ultra-specific activation of CRISPR-Cas12a via sticky-end dsDNA. *Nucleic Acids Res.* **2022**, *50*, 12674–12688.

(45) Cao, G.; Yang, N.; Xiong, Y.; Shi, M.; Wang, L.; Nie, F.; Huo, D.; Hou, C. Completely free from PAM limitations: asymmetric RPA with CRISPR/Cas12a for nucleic acid assays. *ACS Sens.* **2023**, *8*, 4655–4663.

(46) Wang, G. A.; Wu, X.; Chen, F.; Shen, C.; Yang, Q.; Li, F. Toehold-exchange-based activation of aptamer switches enables high thermal robustness and programmability. *J. Am. Chem. Soc.* **2023**, *145*, 2750–2753.

(47) Oesterreich, S.; Davidson, N. The search for ESR1 mutations in breast cancer. *Nat. Genet.* **2013**, *45*, 1415–1416.

(48) Jeselsohn, R.; Bergholz, J. S.; Pun, M.; Cornwell, M.; Liu, W.; Nardone, A.; Xiao, T.; Li, W.; Qiu, X.; Buchwalter, G.; et al. Allele-specific chromatin recruitment and therapeutic vulnerabilities of ESR1 activating mutations. *Cancer Cell* **2018**, *33*, 173–186.

(49) Leventakos, K.; Kipp, B. R.; Rumilla, K. M.; Winters, J. L.; Yi, E. S.; Mansfield, A. S. S768I mutation in EGFR in patients with lung cancer. *J. Thorac. Oncol.* **2016**, *11*, 1798–1801.

(50) Le, X.; Nilsson, M. B.; Robichaux, J. P.; Heymach, J. V. ARTEMIS highlights VEGF inhibitors as effective partners for EGFR TKIs in EGFR mutant NSCLC. *Cancer Cell* **2021**, *39*, 1178–1180.